Applied Thermal Engineering 140 (2018) 476–486

Contents lists available at ScienceDirect

Applied Thermal Engineering

journal homepage: www.elsevier.com/locate/apthermeng

Research Paper

Development of an energy cost prediction model for a VRF heating system

Bo Rang Park[a], Eun Ji Choi[a], Jongin Hong[b], Je Hyeon Lee[c], Jin Woo Moon[a,*]

[a] School of Architecture and Building Science, Chung-Ang University, Seoul, South Korea
[b] Department of Chemistry, Chung-Ang University, Seoul, South Korea
[c] Department of Digital Appliance R&D Team, Samsung Electronics, Suwon, Seoul, South Korea

HIGHLIGHTS

- A predictive and adaptive ANN model was developed for controlling heating system.
- The model predicted heating energy cost for the different variable settings.
- Model optimization was conducted for the accurate and stable prediction.
- The optimized model demonstrated its prediction accuracy within the recommended level.

ARTICLE INFO

Keywords:
Predictive and adaptive controls
Artificial neural network
Heating system
Energy cost
Control model and algorithm

ABSTRACT

This study developed a predictive model using artificial neural network (ANN) to forecast the energy cost for a variable refrigerant flow (VRF) heating system. The energy cost is predicted with the ANN model by considering the set-points for the refrigerant condensation temperature, condenser fluid temperature, condenser fluid pressure, and air handling unit supply air temperature together with past operational data and other climatic data. The predicted energy cost was used as a determinant for the control algorithm to optimize the heating system operation in terms of cost.

The study consisted of three steps: initial model development, model optimization, and performance evaluation. The neural network toolbox in the Matrix laboratory was used to develop the model and conduct the performance tests. For the model training and performance evaluation, data sets were collected in the winter from a test building.

Initial model consisted of a structure that included ten input neurons and a learning method. Then, the optimization process was used to find the optimal structure of the ANN model, which was 1 hidden layer with 15 hidden neurons, while the optimal learning method had a 0.5 learning rate and 0.4 momentum. In the performance evaluation, the optimized model demonstrated its prediction accuracy to be within the recommended level, with 0.8417 r^2 and 4.87% coefficient of variation root mean squared error between the measured and the predicted costs, thus proving its applicability in the control algorithm to supply a comfortable indoor thermal environment in a cost-efficient manner.

1. Introduction

Although the rate of increase in energy consumption by commercial and public buildings is starting to ease, the total energy consumption is still increasing. According to the U.S. Energy Information Administration (EIA), the global primary energy consumption growth rate and CO_2 emission growth rate reached 85% and 75%, respectively, from 1980 to 2012 [1]. The percentage of energy consumption in buildings of the total amount of energy increased from 33.7% in 1980 to 41.1% in 2010 in the U.S and 40% in China from 1990 to 2009. In the European Union (E.U.), building energy consumption accounted for 55% of the total energy in 2012 [2].

Heating energy, which is mainly obtained from gas and electricity, constitutes the largest part of the total energy consumption [3]. In other words, heating energy is the principal factor increasing the world's primary energy consumption [4,5]. Thus, proper system selection and control methods present potentials savings in heating energy consumption, which would reduce greenhouse gas emissions and in turn also reduce the environmental impact [6].

Air conditioning use is increasing in accordance with the demands

* Corresponding author.
E-mail addresses: pbr_1123@naver.com (B.R. Park), ejjchl77@gmail.com (E.J. Choi), hongj@cau.ac.kr (J. Hong), hj8993.lee@samsung.com (J.H. Lee), gilerbert73@cau.ac.kr (J.W. Moon).

https://doi.org/10.1016/j.applthermaleng.2018.05.068
Received 7 September 2017; Received in revised form 26 April 2018; Accepted 16 May 2018
Available online 18 May 2018
1359-4311/

Nomenclature

SA	supply air
RA	returned air
EA	exhausted air
OA	outdoor air
DX	direct expansion
$TEMP_{OUT}$	average outdoor dry-bulb temperature for the last 1 h, ˚C
$TEMP_{IN}$	average indoor dry-bulb temperature for the last 1 h, ˚C
$TEMP_{CF}$	average hot water temperature for the last 1 h, ˚C
$TEMP_{SA}$	average supply air temperature for the last 1 h, ˚C
$AMOUNT_{CF}$	condenser fluid supply amount for the last 1 h, m^3/h
$TEMP_{COND\_SET}$	refrigerant condensation temperature set-point, ˚C
$TEMP_{CF\_SET}$	condenser fluid temperature set-point, ˚C
$PRES_{CF\_SET}$	condenser fluid pressure set-point, kg/cm^2
$TEMP_{SA\_SET}$	air handling unit supply air temperature set-point, ˚C
$LOAD_{HEAT}$	heating load for the last 1 h, kWh
$COST_{ACT}$	energy cost actually measured in the test building [KRW, 1 KRW = 0.0009 USD]
COSTPRED	energy cost for the next 1 h predicted in the ANN model [KRW, 1 KRW = 0.0009 USD]
$ENERGY_{PUMP}$	energy used by the pumps, kWh
$ENERGY_{FAN}$	energy used by the fans, kWh
$ENERGY_{BO}$	energy used by the boiler, kWh
NHL	number of hidden layers
NON	number of output neurons
MO	momentum
LR	learning rate
P_i	ANN predicted value
S_i	numerically simulated value
KRW	Korean won

from residents, who seek comfortable indoor thermal environment. In middle to large-scale high-rise buildings, central air conditioning systems are increasingly adopted as opposed to the individual systems due to energy efficiency and maintenance needs [7]. To ensure more energy efficiency in the system operation, variable refrigerant flow (VRF) systems have been implemented for use in buildings. As shown in Fig. 1, VRF heating systems consist of outdoor units, heat pumps, direct expansion air handling units (AHU), multiple indoor units, and miscellaneous components. The system controls the refrigerant flow to multiple indoor units by passing the expansion valves, which provides individualized temperature control to feasibly satisfy the thermal comfort of each zone.

In particular, VRF systems offer the advantage of responding to the ambient load conditions to create a more stable indoor thermal environment and to reduce the energy consumed during heating by quickly responding to fluctuations in the partial load. In addition, it also offers convenience in terms of the equipment addition and expansion, cost reduction during installation, short construction period, and easy commissioning and maintenance.

Recently, most prior studies on VRF systems have been classified into four types: (1) performance verification of a VRF system through actual measurements and simulations, (2) comparative analysis with existing air conditioning systems, (3) performance evaluation of a VRF system combined with a ventilation system, and (4) energy-efficient operation of a VRF system.

Li et al. [8] conducted a study to verify the performance of a VRF system by comparing simulations and measurement data to support the validity of the EnergyPlus simulation module, which was developed for water-cooled VRF systems. Nine days of comparison between the measurement data and simulation revealed an error rate of 11.3% for the cooling capacity and 15.7% for the power consumption. Similarly, Zhou et al. [9] compared and analyzed the experimental data with EnergyPlus to evaluate the energy performance of the variable refrigerant volume (VRV) air-conditioning system. The mean error between the measured values and the simulation was 25.2–28.3% for the total cooling capacity.

Aynur et al. [10] compared the performance of existing air conditioning systems and VRF systems by evaluating the energy performance of water-cooled VRF and the accuracy of the EnergyPlus simulation. The VRF system showed 27.1–57.9% in energy savings compared to VAV. Li et al. [11] compared and analyzed cooling fan coils, water-cooled VRF and air-cooled VRF systems. The analysis shows that the fan coil system consumes 20% more energy than the water-cooled VRF, and the air-cooled VRF system was 4% less energy-efficient than the water-cooled VRF system.

Kwon et al. [12] studied the performance of the VRF system combined with a ventilation system by analyzing a VRF system and its cooling efficiency factor (CPF) as well as the comfort of the VRF_SCHX (subcooling heat exchanger) system. The simulations showed that the VRF_SCHX system improves the cooling performance factor (CPF) by 8.5% compared to the VRF system, and both systems are suitable to achieve the ASHRAE comfort zone. In addition, Li et al. [13] compared

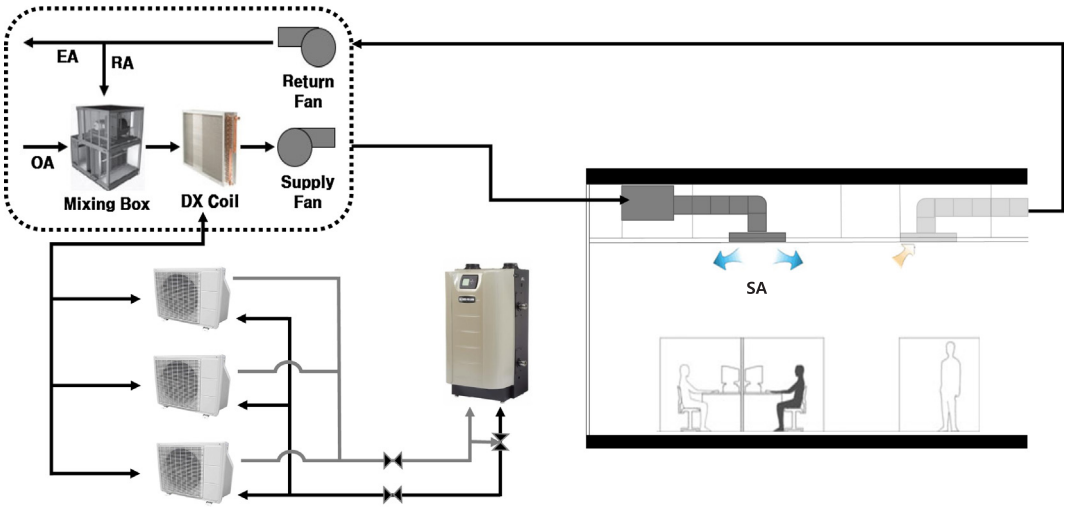

Fig. 1. Diagram of the VRF heating system.

the performance of heat pump-VRF and heat recovery-VRF systems using the computer simulation. The HR-VRF is estimated to achieve 15–17% in energy savings and 6–17% in electricity load reduction compared to the HP-VRF.

Yun et al. [14] investigated the energy-efficient control method of the VRF system by implementing the EnergyPlus Energy Management System (EMS) algorithm to control the refrigerant evaporation temperature. Cooling energy savings of 14% were achieved via higher refrigerant evaporation temperature control.

Although, research is now being conducted on the above topics, there is a lack of research in the energy efficiency and energy cost analysis that take the operating set-point of the VRF system into consideration. To improve energy efficiency, the VRF system control method needs to be further improved for the operating set-point to be properly considered.

So far, the control variables of the VRF system have been determined according to the heuristics of the operator. In general, the supply air temperature set-point ($TEMP_{SA\_SET}$), condenser fluid temperature set-point ($TEMP_{CF\_SET}$), and condenser fluid pressure set-point ($PRES_{CF\_SET}$) are treated as constants that do not take energy efficiency into account. It is therefore necessary to find and apply methods to set more energy-efficient parameters.

To do so, this study developed a predictive model that can forecast the energy cost for the different operating set-points of a VRF heating system. The energy cost for different set-point combinations is compared to find the most cost-effective operating set-points. For this purpose, an ANN model was developed in this study.

The prediction model developed in this study can be applied in the control algorithm. Fig. 2 shows the conceptual flow. The control algorithm to be developed uses the ANN model to obtain the heating energy cost for the various set-points of the control variables. The predicted energy cost from the ANN model will be used as a determinant for optimizing the heating system in terms of cost. The algorithm compares the heating energy cost for each setting and determines the optimum set-point of the control variable. This makes it possible to predict the energy costs for various operations of the heating system. The optimal values of the control variables are applied, and the heating system forms a thermally stable indoor environment that costs less energy.

2. Previous studies regarding ANN-based thermal controls

The study of the ANN is progressing rapidly, and the number of studies to use ANN to predict the conditions of building environments, such as heating systems, indoor air comfort, and ventilation, increased rapidly after 2006 [15]. Moon et al. [16,17] developed ANN models to control the thermal environment in terms of the temperature, humidity, and PMV. In particular, ANN-based algorithm have been proposed to control the openings as well as heating and cooling systems in an integrated manner [18,19]. Garnier et al. [20] proposed a predictive model to control a multizone HVAC system using low-order ANN-based models. Using this algorithm significantly reduced the energy consumption and improved thermal comfort.

Elena et al. [21] investigated an evaluation method to predict the energy consumption of buildings. Although prediction the energy consumption of a building is highly complicated due to a number of influencing factors, including climate, thermal system performance, and occupant patterns, ANN and deep-learning techniques increase the prediction accuracy. Deb et al. [22] conducted a study to predict the cooling energy consumption of an institutional building on a daily basis. In this study, ANN is used for learning and prediction of energy use for the next day, given the previous five days of data. The predicted output is used as an input to predict the next day's results, and repeating this process results in the model having an r^2 value of 0.94 or greater. By using the ANN model, the building energy can be controlled to react instantly.

Sholahudin et al. [23] developed a method to predict the instantaneous building energy load by using various input parameter combinations with a dynamic neural networks model. The Taguchi method used in that study successfully reduced the number of input parameters by identifying the effect of each input parameter. With the reduced number of inputs, the dynamic neural network model can accurately predict the instantaneous heating load.

As a result of numerous studies of ANN applications for the thermal controls of buildings, the accuracy of the prediction and performance has been proven. Nevertheless, a few studies have employed neural networks into VRF systems to control the heating energy consumption. Shi et al. [24] employed an ANN model to detect the operation errors of the VRF system. By using ANN, a high efficiency fault diagnosis model for a VRF system was developed. Chung et al. [25] applied ANN to determine the energy-efficient operating set-points of the VRF cooling system by predicting the cooling energy consumption of the VRF system, and its controllability was verified. However, no study has been conducted to propose a predictive VRF control method in the heating season that also considers costs. Thus, the proper method needs to be developed to achieve a cost-efficient control strategy for VRF systems in the heating season.

3. Development of an ANN-based prediction model

3.1. Factor analysis affecting heating energy consumption

The following variables will be applied in the predictive model for the heating energy cost of a VRF system. The heating energy of the VRF system is mainly consumed in outdoor units, boilers, circulating condenser fluid pumps, and AHU fans. The factors that determine the energy consumption are (1) ambient environmental conditions, and (2) system variable setting values. The ambient environmental conditions of the indoor and outdoor environmental factors, outdoor temperature, and indoor temperature determine the indoor heating energy consumption. To accurately predict the future heating energy, the heating load of the building that was previously measured was selected as one of the input variables of the ANN model, assuming that the heating load in the same building will not change significantly. The heating load was calculated using Eqs. (1) and (2),

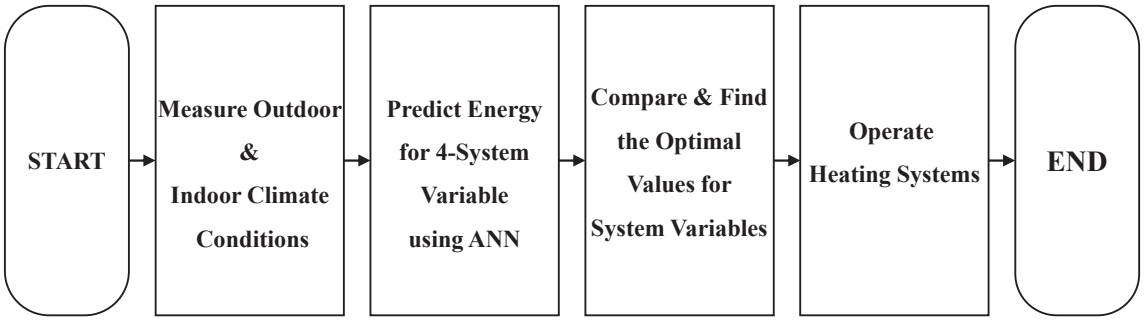

Fig. 2. Thermal control algorithm.

$$LOAD_{HE} = LOAD_{BO} - ENERGY_{OUTUNT} \quad (1)$$

$$LOAD_{BO} = (TEMP_{BOS} - TEMP_{BOR}) \times FR_{CT} \times c_p \times \rho \quad (2)$$

where $LOAD_{HE}$: heating load, kWh; $LOAD_{BO}$: load of the boiler, kWh; $ENERGY_{OUTUNT}$: energy used by the outdoor units, kWh; $TEMP_{BOS}$: condenser fluid supply temperature of the boiler, ˚C; $TEMP_{BOR}$: condenser fluid return temperature of the boiler, ˚C; FR_{CT}: condenser fluid volume flow rate, m^3/h; c_p: specific heat for water, kcal/kg ˚C; and ρ: density of water, kg/m^3.

The system variables are set considering the outdoor units, boiler, pumps to circulate the condenser fluids, and fans of the AHU. Eqs. (3)–(6) show the electric and gas energy consumption by the outdoor units [26,27], boiler, pumps [28], and the fans of the AHU [29,30] respectively. The coefficients in Eqs. (3-1) and (3-5) are derived from both a technical data book [31] and from data obtained from field measurement. Similarly, the coefficients in Eqs. (5) and (6-1) are derived from field measurement data. Those coefficients can only be applied to the particular system that was used in the test building [25], and a detailed description of how the field measurements were derived for the coefficients is given in Section 3.2.1.

$$P_{OUTUNT} = Q_{OUTUNT} \times 1/COP_{REF} \times CAPFT \times EIRFT \times EIRFPLR \times EIRFLPM \times EIRFRC \quad (3)$$

$$CAPFT = 1.4926264835 - 0.01393254X - 0.0001548X^2 \quad (3\text{-}1)$$

$$EIRFT = 0.8002364 + 0.0179363\,X + 0.0009182X^2 - 0.01341544\,Y + 0.00108534Y^2 - 0.0022828XY \quad (3\text{-}2)$$

$$EIRFPLR = 6.025738\,PLR - 22.38675PRI^2 + 31.6677PLR^3 - 14.3232PLR^4 \quad (3\text{-}3)$$

$$EIRFLPM = 1.02503 - 0.000056778CMH \quad (3\text{-}4)$$

$$EIRFRC = -5.3521 + 0.24069RC - 0.00197RC^2 \quad (3\text{-}5)$$

$$BGR = OUER/0.99 \quad (4)$$

$$P_{CT} = -0.00000000001gwlpm^3 + 0.0000008gwlpm^2 - 0.0017gwlpm + 5.5587 \quad (5)$$

$$FF = m/m_{design} \quad (6)$$

$$f_{pl} = 0.0023 + 0.684FF - 1.8832FF^2 + 2.2FF^3 \quad (6\text{-}1)$$

$$Qtot = f_{pl} m_{design} \Delta P/(e_{tot} \rho_{air}) \quad (6\text{-}2)$$

where P_{OUTUNT}: electric power of the outdoor unit, kW; Q_{OUTUNT}: reference capacity of the outdoor unit, kW; COP_{REF}: reference coefficient of performance, 4.787 W/W; CAPFT: heating capacity ratio according to the entering warm fluid and inlet wet-bulb air temperatures, dimensionless; EIRFT: electric input ratio according to the entering warm fluid and inlet wet-bulb air temperatures, dimensionless; EIRFPLR: electric input ratio according to the part load ratio, dimensionless; EIRFLPM: electric input ratio according to the flow rate of warm fluid, dimensionless; EIRFRC: electric input ratio according to the refrigerant condensing temperature, dimensionless; X: inlet air wet-bulb temperature entering the DX coil in the AHU, ˚C; Y: entering warm fluid temperature, ˚C; PLR: part load ratio, %; CMH: flow rate of warm fluid, m/s; RC: refrigerant condensing temperature, ˚C; BGR: boiler gas consumption rate, kWh; OUER: sum of evaporation heat loss of outdoor units, kWh; P_{CT}: electric power of the pumps, kW; gwlpm: amount of warm fluid, liter/minute; FF: flow fraction; m: current air mass flow, kg/s; m_{design}: design(maximum) air flow, kg/s; f_{pl}: fraction of full load power, dimensionless; Q_{tot}: fan power, W; ΔP: fan design pressure increase, Pascal; e_{tot}: fan total efficiency, dimensionless; ρair: air density at standard conditions, kg/m^3.

This equation was used to determine that the supply air temperature of the AHU, flow rate and temperature of the condenser fluid, and refrigerant condensation temperature were important determinants of the energy consumption of the heating system. These values were selected as input variables in the ANN model.

Among the determinants, the boiler gas consumption is directly affected by the outdoor temperature and the condenser fluid temperature setting value, and it is indirectly influenced by the DX coil load. The pump consumption to circulate the condenser fluids is directly affected by the amount of condenser fluid. The power consumption of the AHU fan is affected by the AHU discharge air temperature (supply air temperature $TEMP_{SA}$) because the AHU discharge air temperature has a direct effect on the flow of the air through the AHU fan. Finally, the power consumption of the outdoor unit is directly affected by the condenser fluid flow rate, condenser fluid temperature, DX coil heating load, and indoor air temperature.

The factor analysis highlighted the indoor and outdoor air temperature, AHU supply air temperature, condenser fluid amount and temperature, and refrigerant condensation temperature. The values for these parameters were employed as input variables of the ANN model in Section 3.2.1.

3.2. Process to develop the ANN model

Fig. 3 provides three key steps to develop the ANN model in this study. Developing and validating the ANN model that predicts with greater accuracy and implementing in a control algorithm would make it possible to operate the VRF heating system in a more cost-effective manner. The details of the three key steps are provided below.

The first step is to develop the initial model. The ANN model consisted of the initial configuration and learning methods, and the initial input variables were selected based on the factor analysis conducted in Section 3.1, by which a series of variables relevant to the heating energy consumption were selected as the input neurons of the model.

The next step was to optimize the ANN model. The model parameters, such as the number of hidden layers (NHL), number of hidden neurons (NHN), learning rate (LR), and momentum (MO), were optimized to produce accurate outputs. The optimization was conducted in a combined fashion so that a series of NHLs and NHNs were tested together, followed by a series of LRs and MOs together.

The last step evaluated the performance using the coefficient of determination (r^2). The biggest r^2 was selected after conducting repeated tests between the predicted (Pi) and the simulated (Si) results to find the optimal values. New data sets were used for the performance evaluation. The ANN performance was evaluated in terms of the

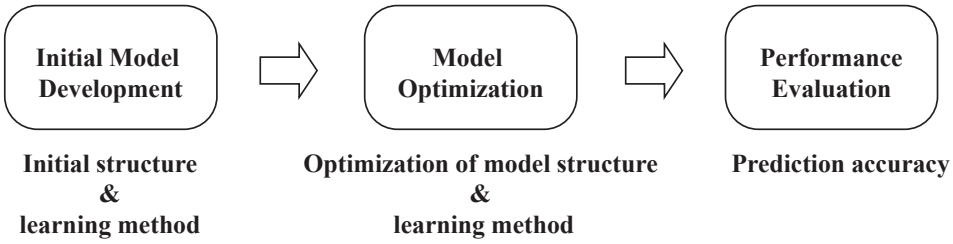

Fig. 3. Development process of the ANN model.

coefficient of determination (r^2), coefficient of variation root mean square error (CVRMSE), and mean bias error (MBE) between the Pi and Si values. The details of each step are as follows:

3.2.1. Initial model development (1st step)

The predictive ANN model, which was employed in this study, conducts the four major processes provided below. Through these processes, the model calculates the designated output and trains itself to produce more accurate results.

(1) Input value and weight: The input values in the ANN model are the input vectors $x_j(where\ j = 1ton,\ n = number\ of\ inputs)$, and the weights connected to each node are the input weight matrix W_{ij}(where i= 1tom,hidden neurons). By multiplying the input values by the weights and summing the bias (b), we form a basic neural network model (a_i).

$$a_j^1 = \sum_{i=1} W_{ji}^1 x_i + \mathrm{b}$$

The hidden layer values are obtained by applying the activation function f to a_j.

$$h_j^1(x,W^1) = f(a_j^1)$$

A sigmoid function, hyperbolic tanh function and ReLU (Rectified Linear Unit) are mainly used as the activation function. To be specific, the sigmoid function converges to 0 or 1 as the value of x becomes smaller or larger, respectively. The equation of the sigmoid function s (x) is as follows.

$$\mathrm{s(x)} = \frac{1}{1 + e^{-x}}$$

The hyperbolic tangent function, tanh(x), has an advantage in that the convergence speed is fast as it has an output range from -1 to 1.

$$\tanh(\mathrm{x}) = \frac{(e^x - e^{-x})}{(e^x + e^{-x})}$$

The ReLU (Rectified Linear Unit) is 0 when the value is below 0, and it works well and has the advantage of being fast to compute [32].

$$\mathrm{ReLU(x)} = \max(0,x)$$

Several types of activation functions can be employed to suit different purposes.

(2) Output value: The value y of the output layer is calculated by activating the function once again using the value of the hidden layer h_j.

$$y(h_j^1,W^2) = f\left(\sum_{j=1} W_j^2 h_j^1\right)$$

(3) Error function: An error function checks the error rate by comparing the predicted value and the actual value. In this case, the error function compares the prediction value (y) with the label value.

$$\mathrm{E} = \sum (prediction\ value - label)^2$$

(4) Optimization: The optimization process is performed to find the case where the error function has the smallest value, and at the same time the accuracy is the highest. The gradient descent method is mainly used to minimize the parameter w of the error function. In the gradient descent method, the gradient (∇E) is used.

$$\nabla\ \mathrm{E} = \frac{\partial E}{\partial w}$$

$$w^{(t=1)} = w^t - \in \nabla \mathrm{E}$$

The parameter w is moved in the direction of ∇E to find the minimum point of w. The learning rate (∈) is an important factor in the training process.

Fig. 4 shows that the initial structure of the ANN model consisting of three structures: the input layer, hidden layer, and output layer. The inputs were selected as variables related to the heating energy cost, as mentioned in Section 3.1. The initial input neurons are comprised of ten variables: (1) average outdoor dry-bulb temperature for the last 1 h ($TEMP_{OUT}$, ˚C); (2) average indoor dry-bulb temperature for the last 1 h ($TEMP_{IN}$, ˚C), (3) average hot water temperature for the last 1 h ($TEMP_{CF}$, ˚C), (4) average supply air dry-bulb temperature for the last 1 h ($TEMP_{SA}$, ˚C), (5) condenser fluid supply amount for the last 1 h ($AMOUNT_{CF}$, m^3/h), (6) refrigerant condensation temperature set-point ($TEMP_{COND\_SET}$, ˚C), (7) condenser fluid temperature set-point ($TEMP_{CF\_SET}$, ˚C), (8) condenser fluid pressure set-point ($PRES_{CF\_SET}$, kg/cm^2), (9) air handling unit supply air temperature set-point ($TEMP_{SA\_SET}$, ˚C), and (10) heating load for the last 1 h ($LOAD_{HEAT}$, kWh).

To use the heating energy cost as an objective function to control the heating system, the total amount of energy consumed is converted to the energy cost [KRW]. The energy cost is composed of both the gas consumption [m3/h] and the power consumption [kWh]. Since the main goal is to quantify the benefits that residents and consumers can gain through the control model, the operating cost is set to an objective function. To calculate the gas consumption of the boiler, the steam calorie and gas consumption were used, as shown in the following Eqs. (7) [32] and (8) [33]. Gas refers to the gas price from Seoul City, Korea while the electricity refers to the electricity tariff of KEPCO (Korea Electric Power Corporation).

$$\mathrm{STEAM_{CAL}} = (\mathrm{TEMP_{CS}} - \mathrm{TEMP_{CR}}) \times \mathrm{FLOW_{COOLANT}} \quad (7)$$

$$\mathrm{GAS_{CON}} = \mathrm{STEAM_{CAL}}/\mathrm{Boiler_{EFFI(99\%)}} \times \mathrm{GAS_{CAL}}(11{,}000\mathrm{kcal/m^3}) \quad (8)$$

where $STEAM_{CAL}$: steam treatment calorie, kcal; $TEMP_{CS:}$ coolant supply temperature, ˚C; $TEMP_{CR}$: coolant return temperature, ˚C; $FLOW_{COOLANT:}$ coolant flow rate, m^3; GAS_{CON}: gas consumption, m^3; $Boiler_{EFFI}$: boiler efficiency, %; $GAS_{CAL:}$ gas calorie, kcal/m_3.

In the initial model, one hidden layer was used to employ hidden neurons based on Eq. (9), which provides the NHN [34,35], where NHN

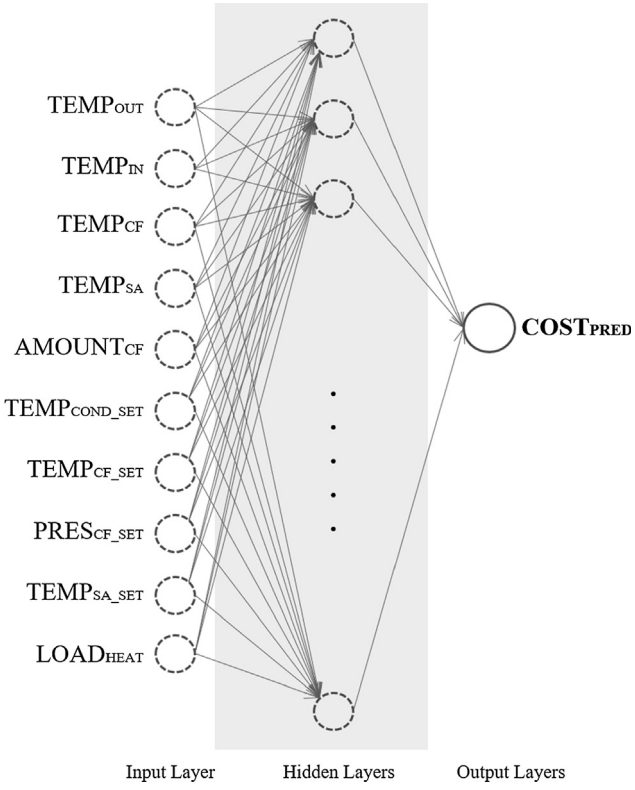

Fig. 4. Initial ANN model.

is the number of hidden neurons, and NIN is the number of input neurons. The NIN is ten, and NHN is twenty-one.

$$NHN = 2NIN + 1 \quad (9)$$

The output neuron represents the predicted energy cost for the next 1 h ($COST_{PRED}$, KRW) in a heating system. The $COST_{PRED}$ refers to the sum of the energy used by the outdoor units ($ENERGY_{OUTUNT}$, kWh), energy used by the boiler ($ENERGY_{BO}$, kWh), energy used by the pumps ($ENERGY_{PUMP}$, kWh), and energy used by the fans in the AHU ($ENERGY_{FAN}$, kWh). The sigmoid function for hidden neurons and the pure-linear function for the output neuron were chosen as transfer functions. The Levenberg-Marquardt algorithm was used as the learning method. The initial LR and MO used values of 0.6 and 0.2, respectively, which concurred with the values obtained in a previous study [36]. The ANN model was then developed using the Neural Network toolbox in MATLAB. In this model, the number of input neurons is ten, and the output neuron is one. Therefore, at least 240 training data sets are required. A total of 619 training data sets were applied in this model based on Eq. (10) [37].

$$N_d = (NHN-(NIN + NON)/2)^2 \quad (10)$$

where NHN: number of hidden neurons; NIN: number of input neurons; NON: number of output neurons.

The entire data set was obtained from an office building as a test building. Fig. 5 shows that the test building is located in Seoul, South Korea, and has a gross floor area of 22,660 m^2. This 10-story office building was constructed in 2015. Monitoring occurred from December 1, 2016 to February 28, 2017, from 9 am to 6 pm on weekdays. The standard floor from the first to the tenth level consists of offices, meeting rooms, and a lobby. The VRF system was used for heating.

Eleven monitoring areas were selected from the low, middle, and high floors. The averages of the data were measured at 5-min intervals, and then averaged for one hour. Table 1 displays the monitoring variables. The actual heating energy data of the target building is based on data collected from the first-floor basement disaster prevention room. The data stored in the integrated building management system (BMS) was collected through sensors installed in the air conditioning system.

Table 1
Measurement variables and the unit of measuring time.

Variables	The unit of measuring time
Outdoor dry-bulb temperature	5 min
Outdoor relative humidity	5 min
Indoor dry-bulb temperature	5 min
Condenser fluid supply temperature of boiler	5 min
Condenser fluid volume flow rates	5 min
Air handling unit supply air temperature set-point	1 h
Condenser fluid temperature set-point	1 h
Condenser fluid pressure set-point	1 h
Energy used cost by the outdoor units	1 h
Energy used cost by the boiler	1 h
Energy used cost by the pumps	1 h
Energy used cost by the fans in the AHU	1 h

3.2.2. Model optimization (2nd step)

This step optimizes the structural variables (Number of Hidden Layers, Number of Neurons) and parameters (Learning Rate and Momentum) of the ANN model. The input value selected through the previous process is used for the optimization. It is necessary to repeat the process to check how the performance of the ANN model changes according to the parameters. The model parameters, such as the NHL, NHN, LR, and MO, are optimized in a coupled fashion. When the first two parameters (i.e., NHL and NHN) were tested to find the optimal numbers, the other two parameters (i.e., LR and MO) were fixed at the initial values (0.5 learning rate and 0.4 momentum). Once the optimal values of the first two parameters were determined, the optimal values were applied, and the next two parameters were tested. After the optimal structural variables of the ANN model are determined, the LR and MO should be determined with the highest prediction accuracy to obtain the optimal parameters. Fig. 6 provides the parametric values that were used to optimize the model.

3.2.3. Performance evaluation (3rd step)

The prediction performance is evaluated in terms of r^2, CVRMSE, and MBE between the P_i and S_i values. The calculation procedure for CVRMSE and MBE is based on Eqs. (11)–(13) [38]. New data sets were collected through optimization, and the ANN model prediction performance was evaluated.

$$RMSE = \sqrt{\sum \frac{(Si-Pi)^2}{N}} \quad (11)$$

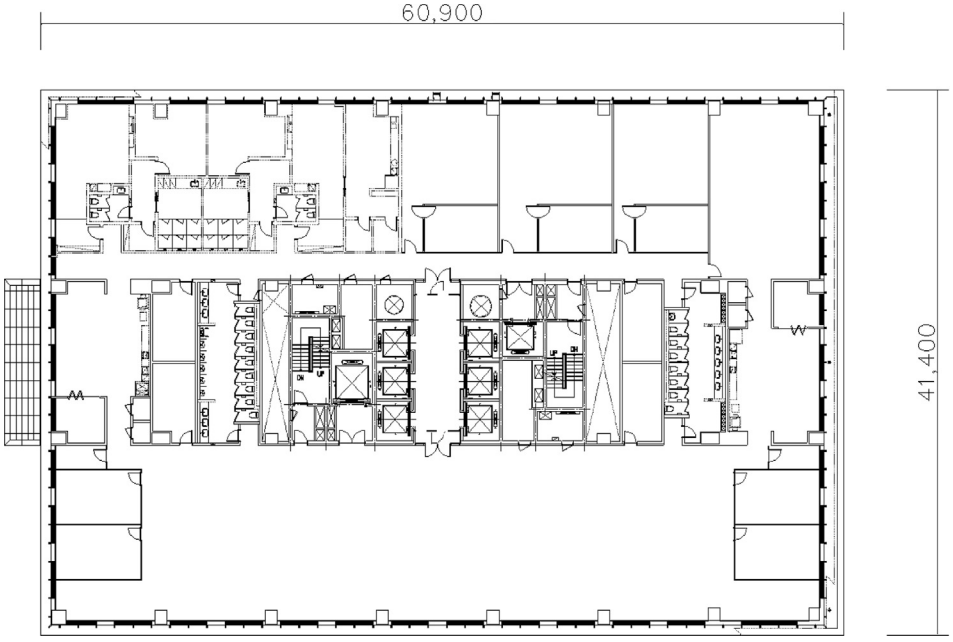

Fig. 5. Typical floor plan of the test building.

55 Cases		NHN			
		15	16	…	25
NHL	1	(NHL_1, NHN_{15})	(NHL_1, NHN_{16})	…	(NHL_1, NHN_{25})
	2	(NHL_2, NHN_{15})	(NHL_2, NHN_{16})		(NHL_2, NHN_{25})
	.	.	.		.
	.	.	.		.
	5	(NHL_5, NHN_{15})	(NHL_5, NHN_{16})		(NHL_5, NHN_{25})

100 Cases		MO			
		0.1	0.2	…	1.0
LR	0.1	($LR_{0.1}$, $MO_{0.1}$)	($LR_{0.1}$, $MO_{0.2}$)		($LR_{0.1}$, $MO_{1.0}$)
	0.2	($LR_{0.2}$, $MO_{0.1}$)	($LR_{0.2}$, $MO_{0.2}$)		($LR_{0.2}$, $MO_{1.0}$)
	.	.	.	…	.
	.	.	.		.
	1.0	($LR_{1.0}$, $MO_{0.1}$)	($LR_{1.0}$, $MO_{0.2}$)		($LR_{1.0}$, $MO_{1.0}$)

Fig. 6. Parametrically tested components and values for ANN optimization.

$$C_V(\text{RMSE}) = \frac{\text{RMSE}}{\text{A}} \times 100 \tag{12}$$

$$\text{MBE} = \frac{1}{\text{n}}\Sigma(\text{Si}-\text{Pi}) \tag{13}$$

where Si is the energy cost predicted by the ANN model ($COST_{PRED}$); Mi is the energy cost actually measured in the test building ($COST_{ACT}$); N is the number of data, and A is the average of the energy cost that is actually measured.

4. Result analysis and discussion

4.1. Predictive model optimization

The optimization step determined the optimal NHL, NHN, LR, and MO of the initial model. When s series of values for the first two parameters (NHL and NHN) were tested, the other two parameters, such as LR and MO, were fixed as in the initial model. The combination presenting the lowest CVRMSE (%) was determined to be the optimal structure.

Fig. 7 presents the summary of the CVRMSE (%) for a series of NHL from 1 to 5, and of NHN from 15 to 25. The total range in the CVRMSE (%) is between 5.53 and 8.27. The lowest CVRMSE value is when NHL is 1 and NHN is 15. Thus, the optimal values for the NHL and NHN are determined as 1 and 15, respectively.

A model that employed the optimal NHL (1) and NHN (15) with varying LR and MO values was developed, and the CVRMSE was compared for each case. The results are presented in Fig. 8. The prediction accuracy was analyzed by increasing the LR and MO from 0.0 to 1.0. When LR is 0.5 and MO is 0.4, the CVRMSE (%) is the least at 4.87. Using this two-step optimization process, the optimized ANN model employed 1 NHL, 15 NHN, 0.5 LR, and 0.4 MO. The final ANN model with the optimized structure and learning methods is provided in Fig. 9.

4.2. Performance evaluation

The performance of the ANN model prediction was evaluated using r^2, CVRMSE, and MBE. The target value is from the ASHRAE Guideline 14 – Measurement, which indicates that an r^2 over 0.8, CVRMSE under 30%, and MBE under 10% can be used to verify the accuracy of the prediction model [39].

Fig. 10 shows the profiles of the measured energy cost (COSTACT)

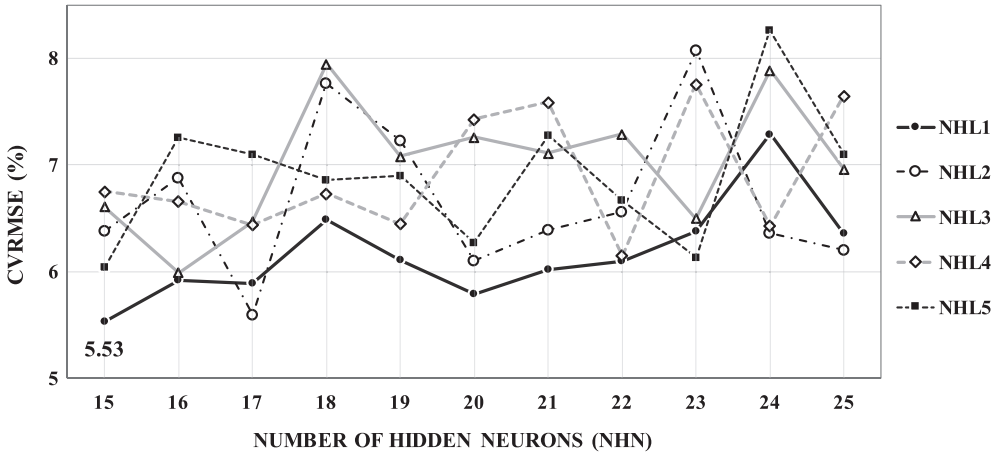

Fig. 7. Graph of CVRMSE (%) for various NHL and NHN values.

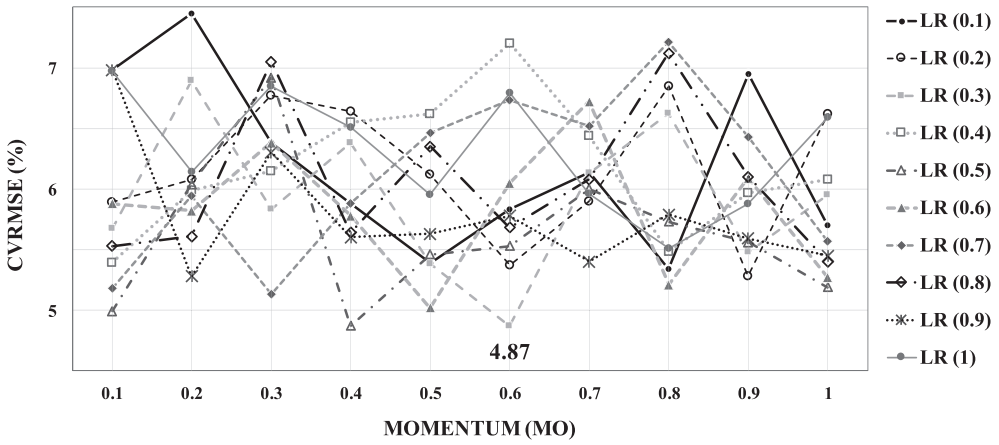

Fig. 8. Graph of CVRMSE (%) for various LR and MO values.

and the predicted cost (COSTPRED). COSTACT and COSTPRED possess a very similar pattern, which verifies the accuracy of the optimized ANN. The linear relationship between the $COST_{ACT}$ from the measurements and $COST_{PRED}$ from the ANN model is shown in Fig. 11 and Table 2**.** Overall, the results of the analysis indicate that $COST_{PRED}$ from the predictions has a strong linear relationship with $COST_{ACT}$ from the measurements. The ANOVA (ANalysis Of VAriance) test results shown in Table 2 indicate that the prediction model was acceptable under a significance level of 0.01. The coefficient of determination (r^2) of the model was 0.8417 in Fig. 11 and Table 2, which is higher than 0.8 as provided by ASHRAE Guideline 14. This result implies that error variance in the $COST_{PRED}$ was reduced by 84.17% when $COST_{ACT}$ was used to predict $COST_{PRED}$. In addition, the CVRMSE (%) between the $COST_{ACT}$ and $COST_{PRED}$ is calculated to be 4.87%, which is less than the target value of 30%. Finally, the MBE (%) is calculated to be 3.75%, which is less than the target value of 10%.

A segmental analysis was conducted to understand the prediction accuracy in further detail. Fig. 12 provides the number of cases and the CVRMSE for the difference between $COST_{ACT}$ and $COST_{PRED}$. Of all cases in the performance evaluation, the forecasting model for CVRMES (%) demonstrated reliable accuracy, giving maximum and minimum values of 13.96% and 1.5%, respectively, which are much lower than the ASHRAE standard of 30%. In particular, 112 out of 150 cases were in the range of error from (−500 to 1000 KRW), and the value of

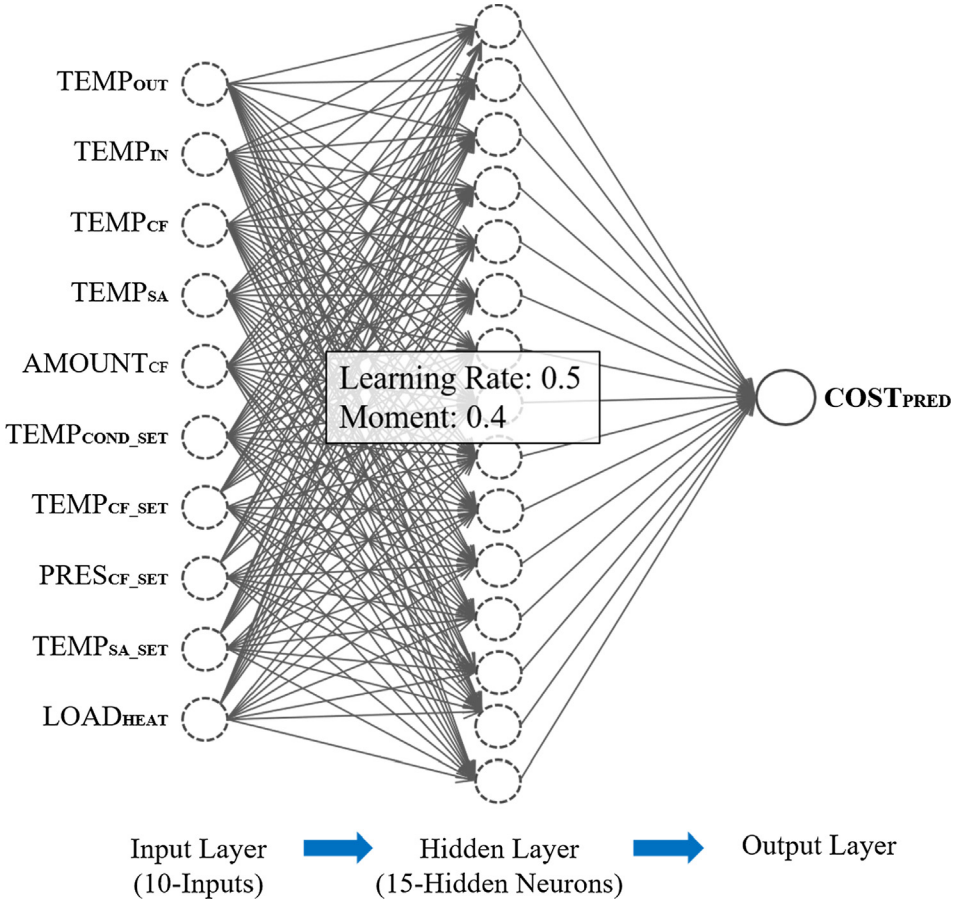

Fig. 9. The Optimized ANN Model.

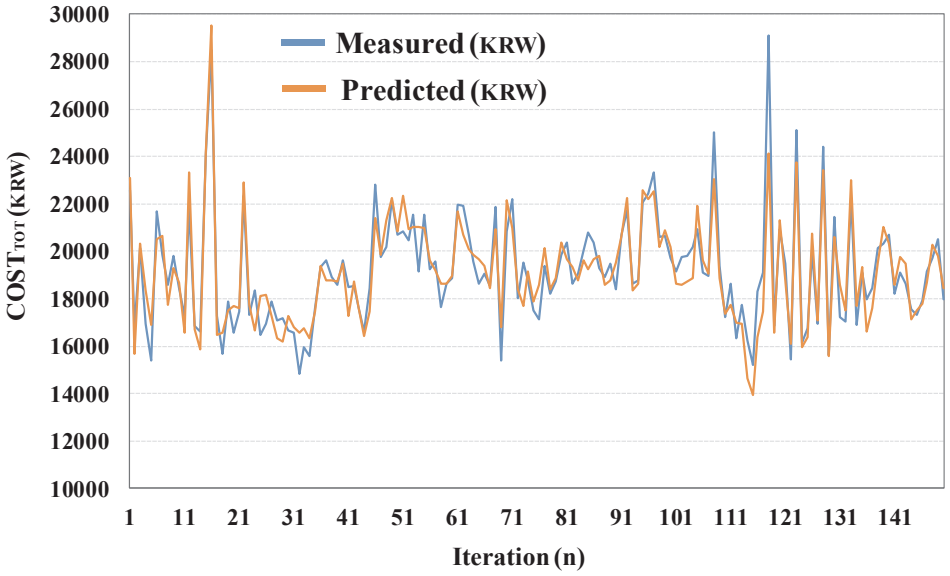

Fig. 10. Comparison of COSTACT and COSTPRED to evaluate the accuracy.

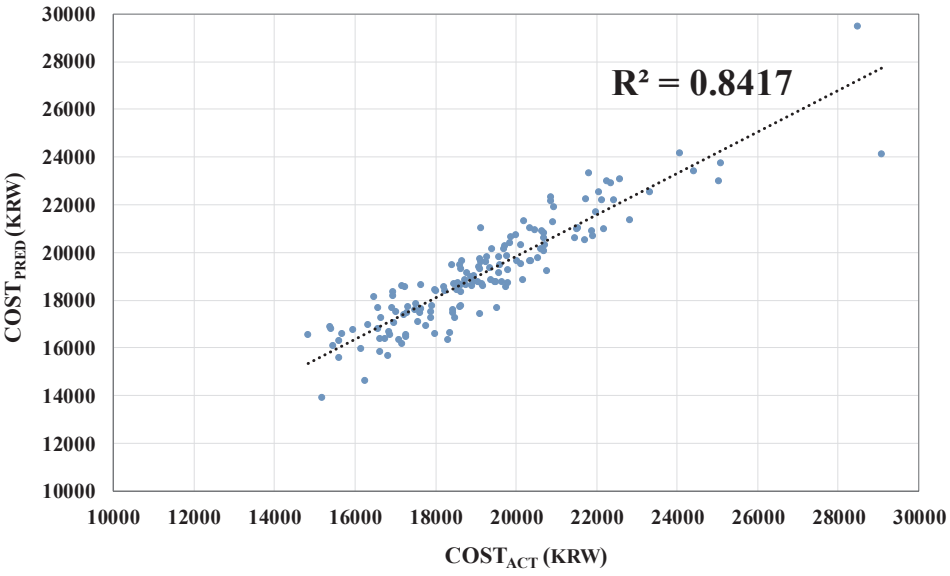

Fig. 11. The coefficient of determination (r^2) Between COSTACT and COSTPRED from the optimized ANN model.

Table 2
ANOVA test result for linear correlation between the difference of $COST_{ACT}$ and $COST_{PRED}$.

	Unstandardized coefficients		t	Sig.	r^2	ANOVA
	B	Std. Error				
(Constant)	2432.701	599.064	4.061	0.000	0.8417	F(1,148) = 786.801, Sig. = 0.000
$COST_{ACT}$	0.870	0.031	28.050	0.000		

CVRMSE was stable from 1.50 to 3.79. On the other hand, cases that the difference was bigger than 2000 KRW occurred two times during the whole performance evaluation. The $COST_{ACT}$ for these two cases were the biggest as 25,034 and 29,090 KRW, respectively, thus the increase of the difference does not seem to be exceptionally unusual.

The accuracy and stability presented in Figs. 10–12 was resulted from the proper function of the ANN model, which was developed through the gradational steps – (1) factor analysis using equations, (2) initial model development, (3) model optimization, and (4) model training and performing. In particular, through the optimization process which was conducted for finding the proper model structure and learning method, the accuracy and stability of the model could have been significantly improved.

4.3. Discussion

This study developed an energy cost prediction model through an optimization process, and its predictive accuracy was verified through performance tests. The error rate and distribution of $COST_{ACT}$ and $COST_{PRED}$ were found to be within a very small range. The error rate of the ANN model in this study presented better or similar results compared to the ANN model developed in the previous study [25], in which the ANN model estimating the amount of electricity consumption of the VRF cooling system was developed, and its prediction accuracy was also analyzed using the error rate such as r^2, CVRMSE, and MBE. The value

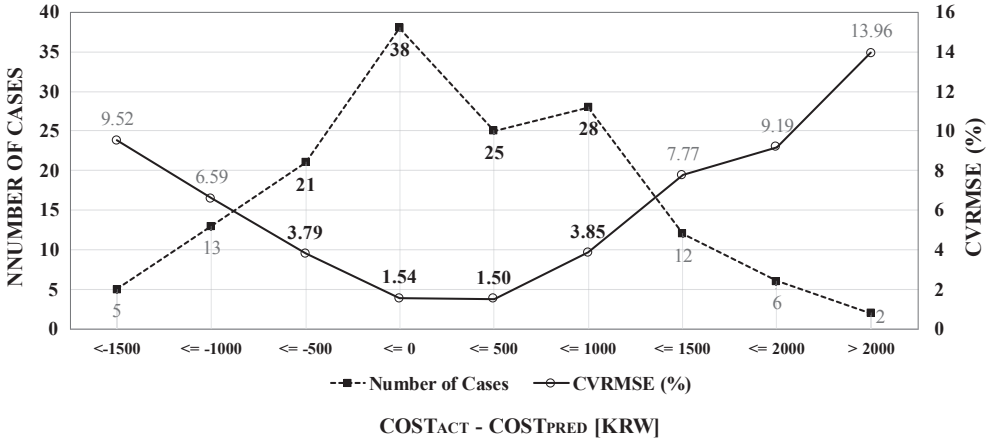

Fig. 12. Number of cases and CVRMSE (%) for difference between COSTACT and COSTPRED cost.

of r^2 is slightly larger as 0.8417 in this study, compared to 0.8137 in the previous study. In addition, the 4.87% value of the CVRMSE in this study is smaller than the 11.28% of the previous study. The MBE of the ANN model in the previous study was −1.18%. A comparison with the ASHRAE standard and the previous study confirmed that the energy cost for VRF heating could be accurately and stably predicted. Based on the performance analysis, the developed ANN model in this study proved its potential for application in the control algorithm for the VRF system.

5. Conclusions

This study developed an ANN-based prediction model to estimate the energy cost by calculating the heating energy consumption when various control parameters of the heating system are set. Development was conducted in three stages: initial model development, model optimization, and performance evaluation. The results of the study can be summarized as follows:

(1) The initial model was designed to have ten input neurons in the input layer, including three exterior and interior thermal conditions and six system operating variables based on the factor analysis relevant to the system energy consumption. Through the optimization process of the initial model, the structure and learning method of the least CVRMSE were found to be 1 NHL, 15 NHN, 0.5 LR, and 0.4 MO. Therefore, the model was optimized to use these values for the structure and learning method.
(2) Through performance tests of the optimized model using r^2, CVRMSE, and MBE, the predicted values of the ANN model were very similar to those measured from the field. The r^2 value was 0.8417 over the standard value of 0.8 provided by ASHRAE Guideline 14. The CVRMSE and MBE were 4.87% and 3.75%, respectively, which were less than the target value of 30% and 10%. The accuracy of the model proved its applicability in the control algorithm.
(3) In addition, the error analysis in the CVRMSE between $COST_{ACT}$ and $COST_{PRED}$ proved the stability of the prediction results. The analysis revealed the maximum CVRMSE was 13.96%, which is significantly lower than the ASHRAE standard of 30%. For most of the cases (112 out of 150), the difference between the $COST_{ACT}$ and $COST_{PRED}$ was in the error range of −500 to 1000 KRW. The results of the error analysis between $COST_{ACT}$ and $COST_{PRED}$ also demonstrated the suitability of the of the developed ANN model.

The results of the analysis regarding r^2, CVRMSE, and MBE between P_i and S_i indicate that the suggested ANN model properly predicts the heating energy cost for different combinations of the system operation variables. In addition, the results of the CVRMSE (%) analysis for the error between $COST_{ACT}$ and $COST_{PRED}$ indicate that the performance of the ANN model is stable. Based on the prediction accuracy, the model was demonstrated to be suitable for application in the control algorithm for optimal operation of a heating system.

Using the control algorithm with the predictive model, the VRF system could be controlled in a cost-effective manner by applying the optimal set-points for the refrigerant condensation temperature, condenser fluid temperature, condenser fluid pressure, and air handling unit supply air temperature. The operating performance of the control algorithm needs to be compared to that of the conventional control method that uses fixed operational set-points. The comparative tests using the field applications and computer simulations will present the pros and cons of each control method in terms of cost, energy, environmental impact, system failure, deterioration, etc.

In addition, the adaptability of the control algorithm embedding the developed ANN model should be studied. The cost of gas and electricity is changing all the time, so the energy cost for a VRF heating system that consumes both gas and electricity varies. The optimal set-point combination for the operating parameters could also change when the ANN model trained using data sets from past conditions does not correspond well to the current energy cost conditions. Thus, the ANN model, which employed the sliding window method to manage training data sets, and the control algorithm need to clearly demonstrate adaptability to changing conditions. The predictive accuracy and stability of the ANN model and the cost effectiveness of the control algorithm will support the adaptability of the proposed VRF control method.

Based on the further studies on the operational performance and adaptability, the control algorithm embedding the developed predictive model in this study will prove its applicability over conventional control strategies.

Acknowledgement

This research was supported by a grant (code 18CTAP-C129762-02) from Infrastructure and Transportation Technology Promotion Research Program funded by Ministry of Land, Infrastructure and Transport of Korean government and the Chung-Ang University Graduate Research Scholarship in 2017.

Appendix A. Supplementary material

Supplementary data associated with this article can be found, in the online version, at http://dx.doi.org/10.1016/j.applthermaleng.2018.05.068.

References

[1] U.S.E.I. Administration, International Energy Outlook 2013, 2013.
[2] D. Bosseboeuf, Energy Efficiency Trends and Policies in the Household and Tertiary Sectors An Analysis Based on the ODYSSEE and MURE Databases, 2015.
[3] C. Xiaodong, D. Xilei, L. Junjie, Building energy-consumption status worldwide and the state-of-the-art technologies for zero-energy buildings during the past decade, Energy Build. 128 (2016) 198–213.
[4] Climate Change 2014: Mitigation of Climate Change, IPCC, 2014.
[5] Y.C. Kim, W.H. Hong, Y.L. Zhang, B.H. Son, Y.K. Seo, J.H. Choi, Estimating the additional greenhouse gas emissions in korea: focused on demolition of asbestos containing materials in building, Environ. Res. Public Health 13 (2016).
[6] V. Bianco, D. Righi, F. Scarpa, L.A. Tagliafico, Modeling energy consumption and efficiency measures in the Italian hotel sector, Energy Build. 149 (2017) 329–338.
[7] J.W. Kim, J.H. Park, J.H. Jeong, D.S. Song, A development of a simulation module to analyze the HVAC system performance in office building, Archit. Inst. Korea 29 (2009) 797–800.
[8] Y.M. Li, J.Y. Wu, S. Shiochi, Experimental validation of the simulation module of the water-cooled variable refrigerant flow system under cooling operation, Appl. Energy 87 (2010) 1513–1521.
[9] Y. Zhu, X. Jin, Z. Du, B. Fan, X. Fang, Simulation of variable refrigerant flow air conditioning system in heating mode combined with outdoor air processing unit, Energy Build. 68 (2014) 571–579.
[10] T.N. Aynur, Y. Hwang, R. Radermacher, Simulation comparison of VAV and VRF air conditioning systems in an existing building for the cooling season, Energy Build. 41 (2009) 1143–1150.
[11] Y.M. Li, J.Y. Wu, S. Shiochi, Modeling and energy simulation of the variable refrigerant flow air conditioning system with water-cooled condenser undercooling conditions, Energy Build. 41 (2009) 949–957.
[12] L. Kwon, Y. Hwang, R. Radermacher, B. Kim, Field performance measurements of a ASHP system with sub-cooler in educational offices for the cooling season, Energy Build. 49 (2012) 300–305.
[13] Y.M. Li, J.Y. Wu, Energy simulation and analysis of the heat recovery variable refrigerant flow system in winter, Energy Build. 42 (2010) 1093–1099.
[14] G.Y. Yun, et al., Development and application of the load responsive control of the evaporating temperature in a VRF system for cooling energy savings, Energy Build. 116 (2016) 638–645.
[15] G. Zhang, B.E. Patuwo, M.Y. Hu, Forecasting with artificial neural networks: the state of the art, Int. J. Forecasting 14 (1) (1998) 35–62.
[16] J.W. Moon, J. Kim, ANN-based thermal control models for residential buildings, Build. Environ. 45 (2010) 1612–1625.
[17] J.W. Moon, J.D. Chang, S. Kim, Determining adaptability performance of artificial neural network-based thermal control logics for envelope conditions in residential buildings, Energies 6 (2013) 3548–3570.
[18] J.W. Moon, Comparative performance analysis of the artificial-intelligence-based thermal control algorithms for the double-skin building, Appl. Therm. Eng. 91 (2015) 334–344.
[19] J.W. Moon, Development of integrated control methods for the heating device and surface openings based on the performance tests of the rule-based and artificial-neural-network-based control logics, KIEAE J. 14 (2014) 97–103.
[20] I.D. Basheer, M. Hajmeer, Artificial neural networks: fundamentals, computing, design, and application, J. Microbiol. Meth. 43 (2000) 3–31.
[21] E. Mocanu, P.H. Nguyen, M. Gibescu, W.L. Kling, Deep learning for estimating building energy consumption, Sustain. Energy Grids Networks 6 (2016) 91–99.
[22] C. Deb, L.S. Eang, J. Yang, M. Santamouris, Forecasting diurnal cooling energy load for institutional buildings using Artificial Neural Networks, Energy Build. 121 (2016) 284–297.
[23] S. Sholahudin, H. Han, Simplified dynamic neural network model to predict heating load of a building using Taguchi method, Energy (2016) 1–7.
[24] S. Shi, G. Li, H. Chen, J. Liu, Y. Hu, L. Xing, W. Hu, Refrigerant charge fault diagnosis in the VRF system using Bayesian artificial neural network combined with Relief filter, Appl. Therm. Eng. 112 (2017) 698–706.
[25] M.H. Chung, Young Kwon Yang, Kwang Ho Lee, Je Hyeon Lee, Jin Woo Moon, Application of artificial neural networks for determining energy-efficient operating set-points of the VRF cooling system, Build. Environ. 125 (2017) 77–87.
[26] The U.S. D.O.E., EnergyPlus Engineering Reference V. 8.5; The Reference to EnergyPlus Calculations, Chapter 15.11.1 Variable Refrigerant Flow Heat Pump Model (System Curve Based Model), 2011. p. 1121.
[27] Samsung Electorincs Co., DVM S Water Technical Data Book, 2015.
[28] The U.S. D.O.E., EnergyPlus Engineering Reference V. 8.5, The Reference to EnergyPlus Calculations, Chapter 15.17.3 Variable Speed Pump, 2011, pp. 1257.
[29] The U.S. D.O.E., EnergyPlus Engineering Reference V. 8.5, The Reference to EnergyPlus Calculations, Chapter 15.9.2.3 Simulation, 2011, p. 1015.
[30] The U.S. D.O.E., EnergyPlusInputOutput Reference V. 8.5; The Reference to EnergyPlus Calculations, Chapter 1.41.3 Fan: VariableVolume, 2011, p. 1907.
[31] Samsung Electronics Co, DVM S Water Technical Data Book, 2015.
[32] G. Aurelien, Hands-On Machine Learning with Scikit-Learn & TensorFlow, first ed, O'Reilly Media, Inc, Sebastopol (CA), 2017.
[33] Seoul City Gas Co., Gas price table, 2017.
[34] Korea Electric Power Corporation Co., Electricity price table, 2017.
[35] D. Datta, S.A. Tassou, D. Marriott, Application of neural networks for the prediction of the energy consumption in a supermarket. In: CLIMA 2000, Brussels (Belgium), 1997. p. 98–107.
[36] J. Yang, H. Rivard, R. Zmeureanu, On-line building energy prediction using adaptive artificial neural networks, Energy Build. 37 (2005) 1250–1259.
[37] J.W. Moon, K. Kim, H. Min, ANN-based prediction and optimization of cooling system in hotel rooms, Energies 8 (2015) 10775–10795.
[38] S.A. Kalogirou, M. Bojic, Artificial neural networks for the prediction of the energy consumption of a passive solar building, Energy 25 (200l) 479–91.
[39] American Society of Heating, Refrigerating, and Air-Conditioning Engineer. ASHRAE Guideline14-Measurement of energy and demand savings. ASHRAE Inc., 2002.